Natural Science Report, Ochanomizu University, Vol. 12, No. 2, 1961
お茶の水女子大学 自然科学報告 第12巻 第2号

Hot-Wire Investigations of Smoke Patterns Caused by a Spherical Roughness Element

Masako Mochizuki (望月昌子)

Department of Physics, Faculty of Science,
Ochanomizu University, Tokyo

Abstract

The transition process from laminar to turbulent flow caused by a sphere placed on a flat plate has been investigated using smoke technique in detail by the author. These results are compared with those obtained in the present paper using hot-wire method.

From the measurements of mean wind velocity, it is found that the smoke filaments appearing behind the sphere exhibit the central part of the longitudinal vortices in the case of low wind velocity and non-turbulent flow. As the turbulence wedge appears, there exists a longitudinal vortex close to the plate along the boundary of the wedge.

In the case when clear periodic vortices appear, the wave forms of the velocity fluctuations are observed at various three dimensional positions of hot-wire relative to the vortices, taking simultaneously photographs of the smoke patterns and hot-wire position using movie camera. From the results of these observations, it is found that the longitudinal vortices act to transfer the fluid up and down and the equalization of wind velocity takes place in the wake of the sphere by the vortices which exist there.

Introduction

The flow patterns caused by a sphere in a boundary layer on a flat plate have been previously observed using smoke techniques[1]. When wind velocity is small, a pair of smoke spirals appears just behind the sphere and two parallel smoke filaments trail downstream parallel to the plate from the top of the spiral vortices (we may call them trailing vortices). At the same time, a horseshoe-shaped filament is formed which circles round the upstream side of the sphere and then flows downstream behind the sphere (we may call it horseshoe vortex) (Fig. 1). As the wind velocity increases, the trailing vortex filaments begin to oscillate very slightly, becomming at higher velocities to show protuberances in pairs arranged at constant interval. At still high velocities those parts gradually become strongly twisted and stretched upward,

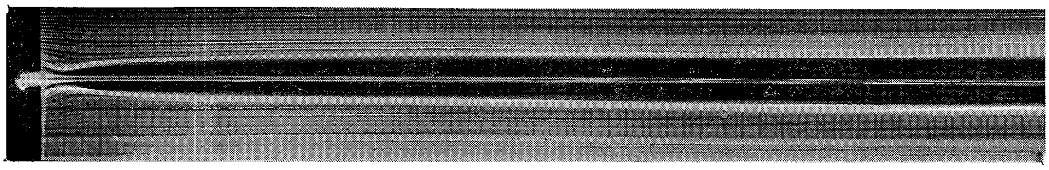

(a) $U=0.9$ m/sec, $k=0.7$ cm, $x_k=20$ cm
The first stage

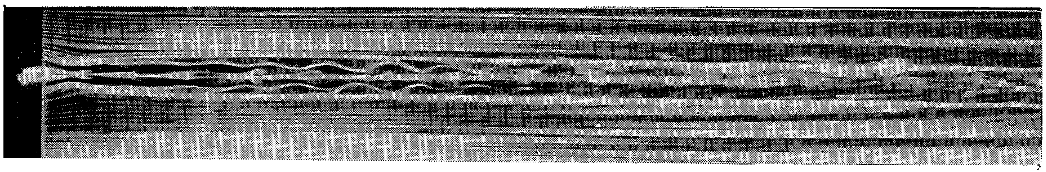

(b) $U=1.3$ m/sec, k=0.71 cm, $x_k=20$ cm
The second stage

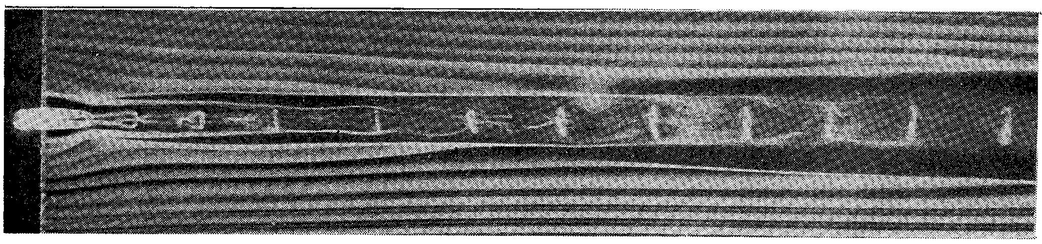

(c) $U=5.1$ m/s $k=0.33$ cm, $x_k=50$ cm
The second stage

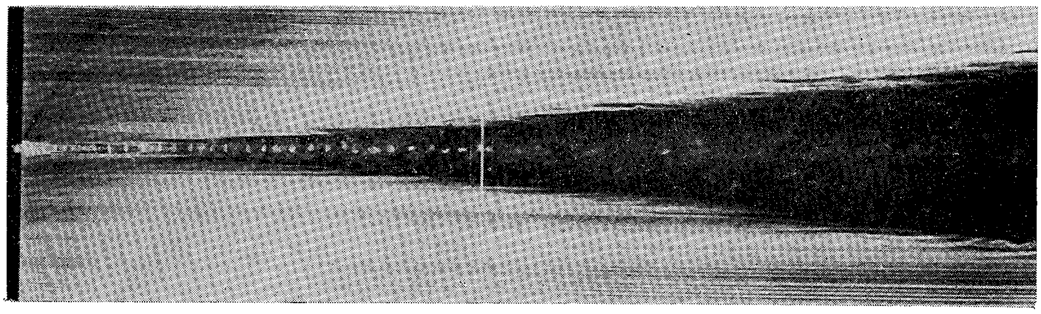

(d) $U=8.3$ m/sec, $k=0.23$ cm, $x_k=50$ cm
The third stage

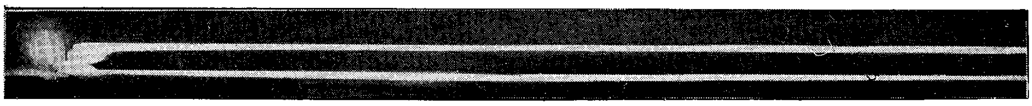

(e) Side view of the first stage

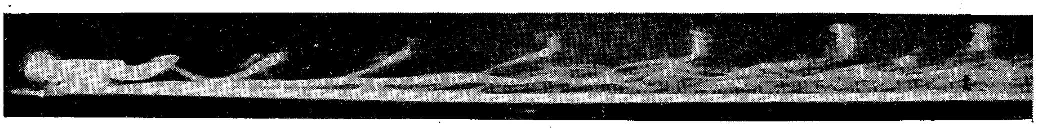

(f) Side view of the second stage

Fig. 1. Smoke patterns in each stage.

until they finally form arch-shaped vortices. At low velocities, the horseshoe vortex filament is very close to the plate downstream of the sphere, and their downstream parts rise as the wind velocity increases, then their forms change periodically due to the influence of periodic motion of the trailing vortex filaments. At higher velocities, the flow becomes turbulent from downstream and the turbulence wedge is formed.

There have been many works[2),3)] which investigated the mechanism of turbulent phenomena in detail using hot-wire anemometer, and there also have been many experiments[4),5),6)] by visual observation. In almost all cases, the hot-wire method has been used in the wind tunnel measurement, while the visualization method has been used in the water channel observation. So it was difficult to compare in detail the results obtained by respective method. The hot-wire method and the visualization method have their characteristic properties respectively. The visualization method can show the flow state of a wide region at the same time and indicate objectively the position and the singularity of the existing peculiar flows. But it has not yet been elucidated, what is implied practically by smoke patterns and in which position of the flow does the smoke assemble itself. By adopting both methods in the same time, much more informations may be obtained.

Therefore, we planed to investigate the correspondence between the results of smoke and hot-wire method. Namely the flow which has been observed formerly by smoke method was measured by hot-wire method, and moreover, took at the same time the photographs of the smoke patterns and the wave forms of the fluctuations of the wind velocity.

Symbols

x distance measured along plate surface downstream from leading edge
y distance normal to surface, measured from surface
z spanwise direction perpendicular to x-, y-plane
U mean velocity in free stream
$\overline{u}$, $\overline{v}$, $\overline{w}$ mean velocities in x-, y- and z-directions, respectively
u', v', w' velocity fluctuations in x-, y- and z-directions, respectively
x_H distance from leading edge to hot-wire
x_k distance from leading edge to sphere
k diameter of sphere
h_H height of hot-wire position from surface

Method of experiment

Main apparatuses were the same to those which have been used in the former experiment.[1)] The wind tunnel used was a $50 \times 50 \times 200$

cm closed Göttingen-type in our University. A laminar boundary layer was formed on a flat plate which was placed horizontally at a distance of 15 cm above the bottom of the tunnel. The plate was made of black-enameled aluminum and black acryl resin to get good photographic effect, and it was divided into 2 or 3 parts in order to emit the smoke from the gaps. The arrangement is shown in Fig. 2. In order to

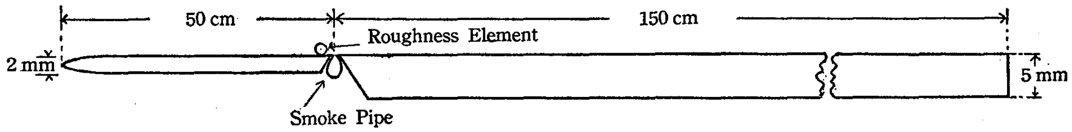

Fig. 2. Experimental arrangement.

regulate the flow for zero pressure gradient, wire gauzes were stretched across above the plate at the downstream end of the measuring section.

As the roughness element, a bearing ball was used, whose diameter (k) was 0.71, 0.55, 0.33 and 0.23 cm, respectively. In the present experiments, the sphere of 0.71 cm in diameter was chiefly used to make the phenomena more distinctly. The sphere was placed on the plate about a half diameter upstream from the smoke source.

The wind velocity was measured by a hot-wire anemometer. A platinum wire 5 μ in diameter and 1 mm in length was used as a sensing part and it was inserted as an arm in a bridge circuit. The mean wind velocity was determined by measuring the out-put of the bridge circuit with a D. C. ammeter and the wave form was observed by a cathode ray oscillograph after amplifying by a D. C. pre-amplifier. The out-put of the amplifier was proportional to the wind velocity within the range of the present experiment. The highest gain of the over-all amplification was 90 db. In all cases the hot-wire was placed perpendicularly to the main flow and parallel to the plate, therefore, only the main stream component of the wind velocity was measured.

In order to determine the instantaneous positions of the hot-wire relative to the smoke patterns when the wave forms of the wind velocity are measured, we took the photograph of the flow patterns together with the hot-wire by a movie camera equipped with a stereo-attachment. A xenon discharge tube was used as a light source which was made to synchronize with the shutter of the movie camera. The flashing light was converted into electric pulse by a photo-voltaic cell and this pulse and the out-put of the hot-wire circuit were put into each element of a dual beam cathode ray oscillograph. These patterns were recorded by a continuous recorder together with time marks. Comparing the oscillograms with the pictures of the movie camera, we can determine which pattern of the velocity fluctuations corresponds to the three dimensional position of the smoke patterns.

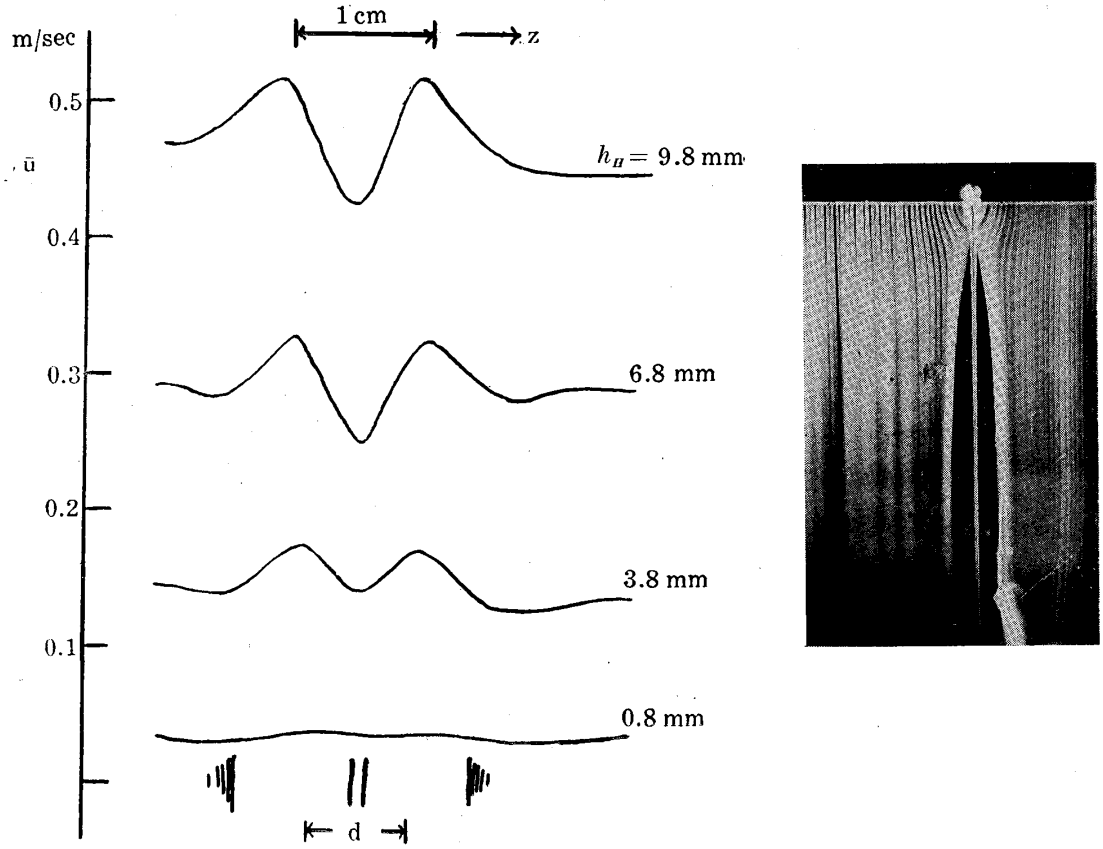

(a) $x_H - x_k = 11$ cm, $U = 0.6$ m/sec

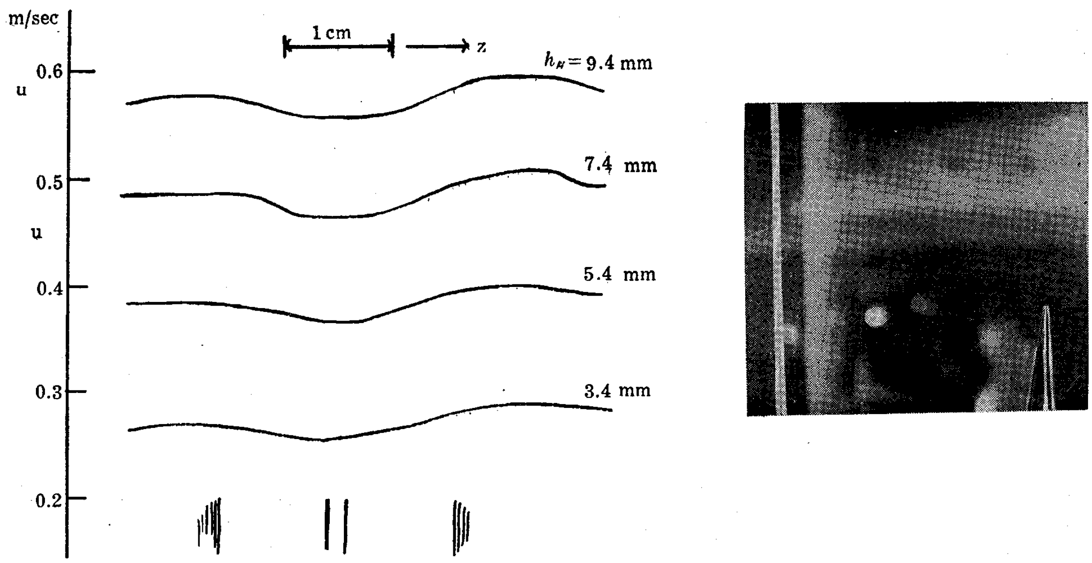

(b) $x_H - x_k = 9.3$ cm, $U = 0.8$ m/sec

Fig. 3. Mean velocity profiles. Center of eddy is at $h_H = 6.8$ mm

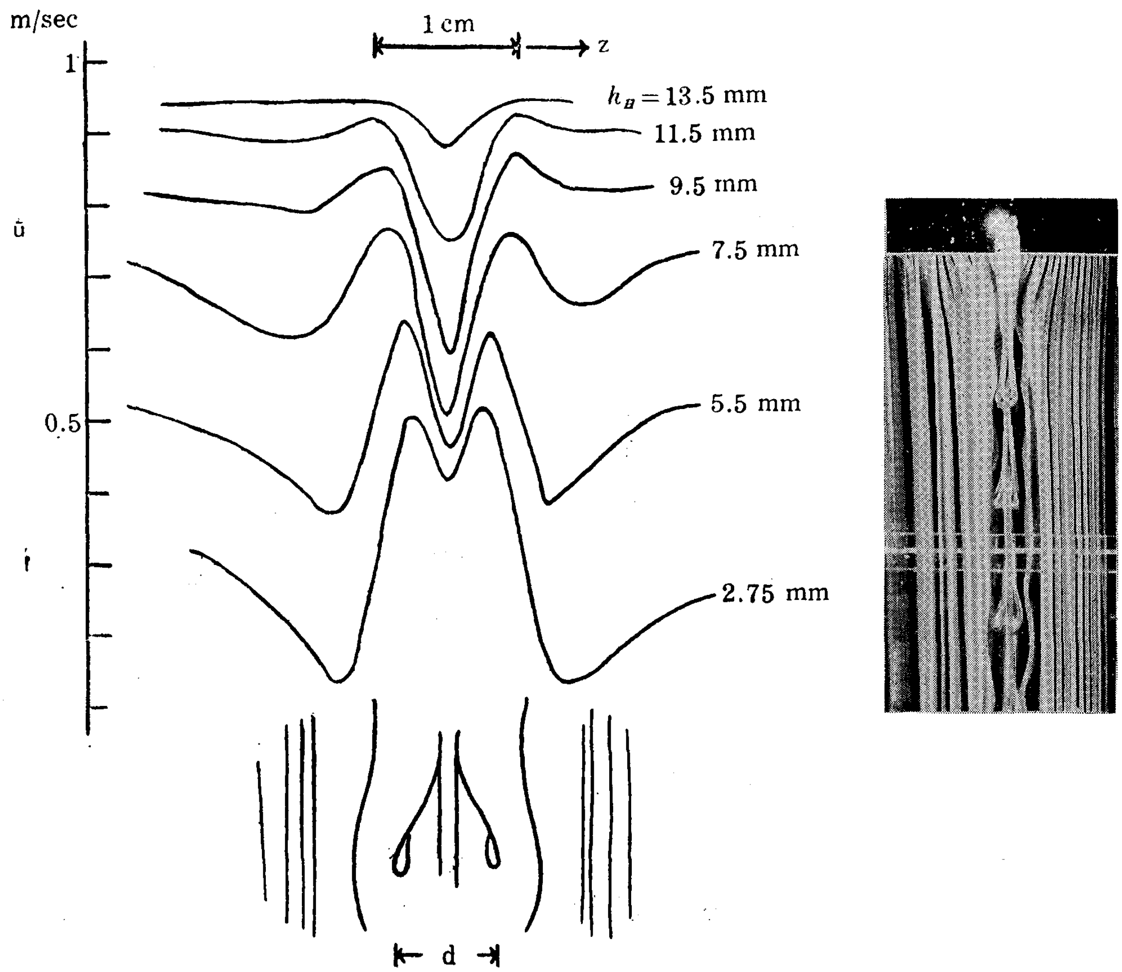

(a) $x_H - x_k = 9$ cm, $U = 1.1$ m/sec

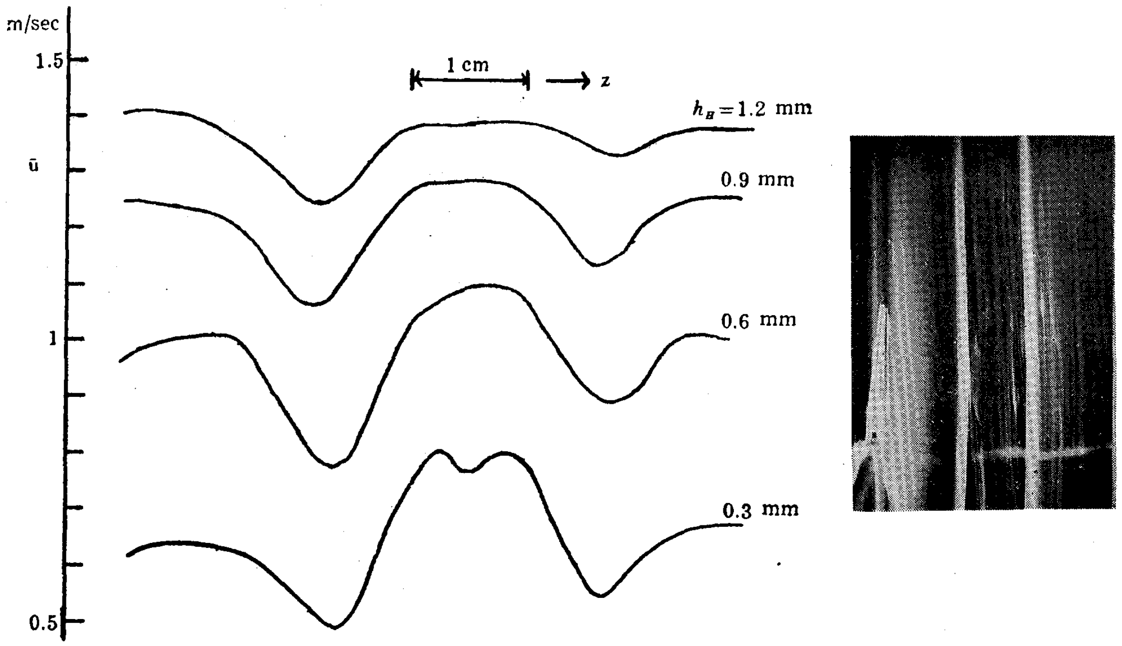

(b) $x_H - x_k = 93$ cm, $U = 1.4$ m/sec

Fig. 4. Mean velocity profiles.

Mean velocity profile and smoke pattern

It has been already reported[1] that the flow caused by the spherical roughness element in a laminar boundary layer along a flat plate changes its patterns as the wind velocity increases. There are three typical stages. The first stage occurs when the wind velocity is low, namely there appear two straight trailing vortex filaments behind the sphere and one horseshoe vortex filament which circles round the sphere (Fig. 1 (a) and (e)). In the second stage, there appear periodically distinct vortices (Fig. 1 (b), (c) and (f)). In the last stage, the turbulence wedge appears (Fig. 1 (d)).

At first, the mean velocity profiles for these three stages were measured by the hot-wire anemometer and the significances of the flow patterns were considered. The measurements were made by transversing horizontally in every 1 mm the hot-wire at several heights and in several

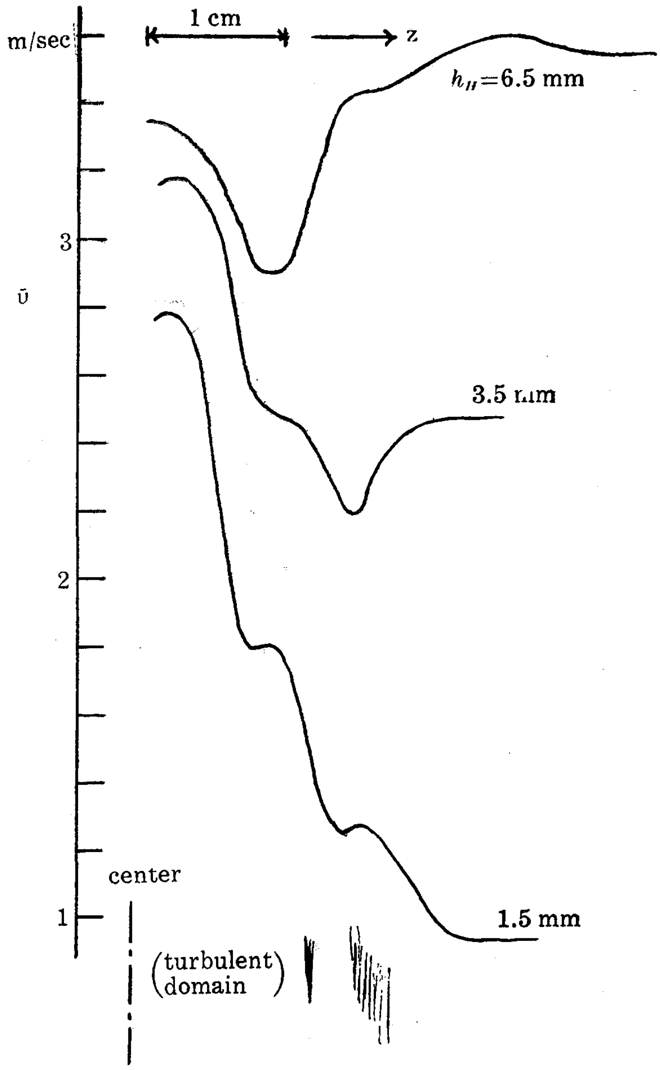

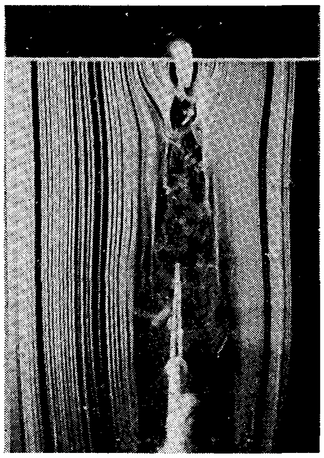

(a) $x_H - x_k = 11$ cm

downstream positions.

The results are shown in Fig. 3 to Fig. 6. In order to make clear the correspondence between the velocity profiles and the smoke patterns, the photographs of the smoke patterns for each case are put on one side and the schematic pictures are put at the bottom.

As it has been pointed out by Schubauer,[7] there may be the waviness of mean velocity in z-direction in boundary layer which is inherent to each wind tunnel. In our wind tunnel, the wave length of that waviness was about 3 cm and the ratio of its amplitude to the mean velocity was about 0.15. In this paper, the effects of these local changes of the mean velocity on the phenomena to be considered were neglected. But in some cases the profiles of the mean velocity downstream of the sphere were calculated by subtracting the amounts of the local change of the velocity from the directly observed data. The resulted profiles were able to show clearly the characteristic features of the results of the present measurement. Fig. 5 shows these corrected profiles.

The velocity profiles and corresponding smoke patterns in the first

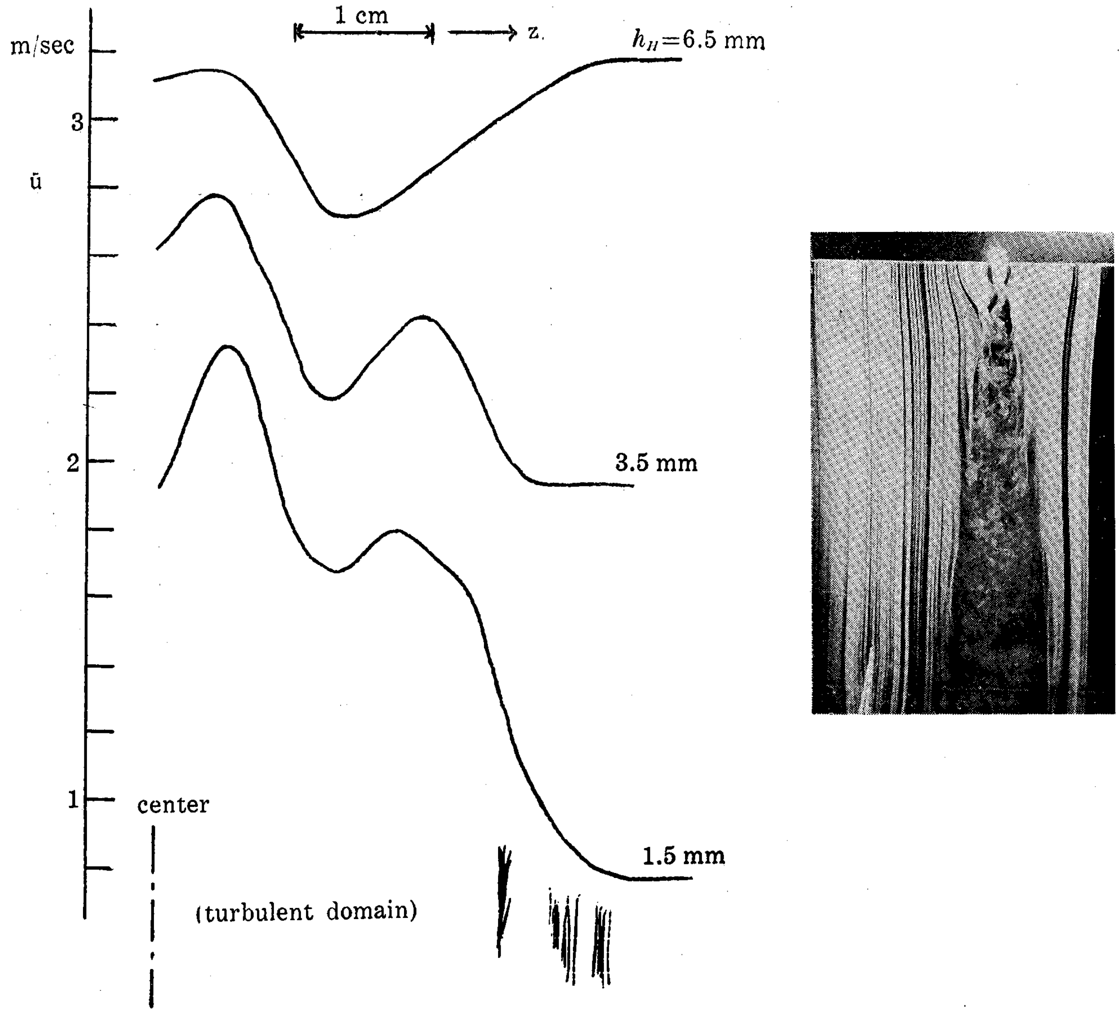

Fig. 5. (b) $x_H - x_k = 22.3$ cm

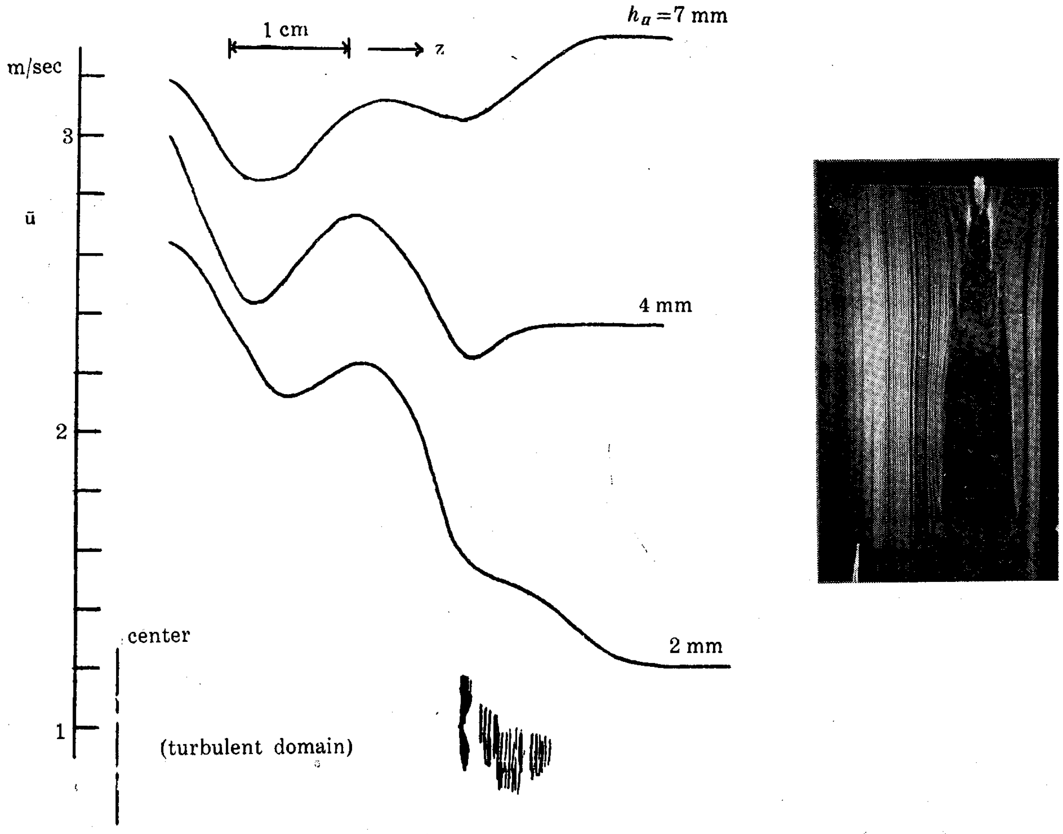

(c) $x_H - x_k = 29$ cm

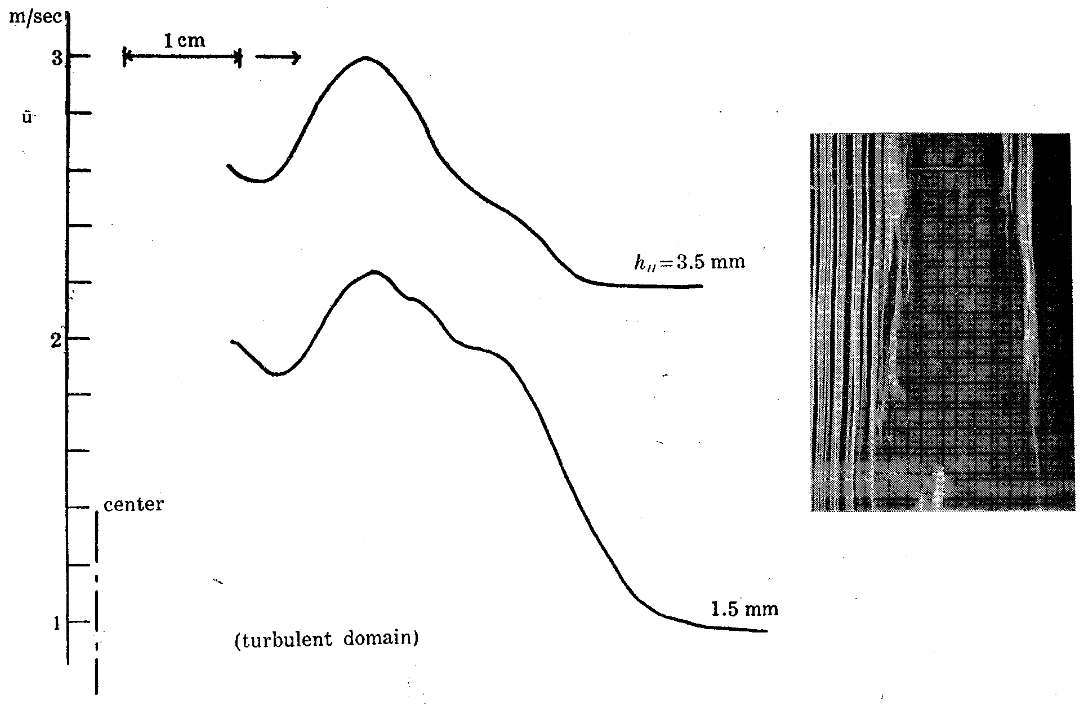

(d) $x_H - x_k = 42.5$ cm

Fig. 5. Mean velocity profiles. $U = 3.9$ m/sec

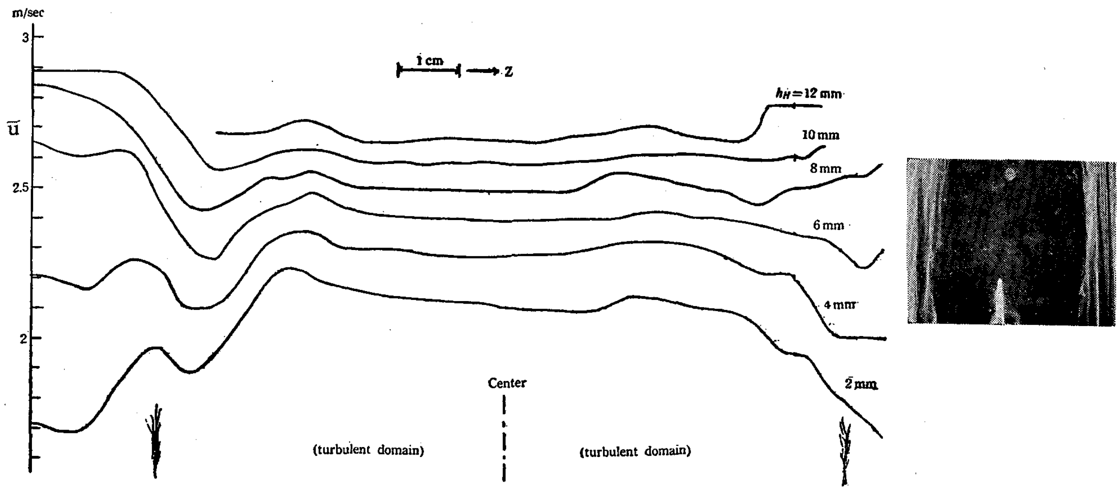

$x_H - x_k = 93$ cm, $U = 2.7$ m/sec

Fig. 6. Mean velocity profiles.

stage are shown in Fig. 3. In the visual observation formerly made, the trailing vortex filaments and the horseshoe vortex filament were recognized, and these filaments were noticed to show the centers of these vortices and, in some cases, even their rotating directions were recognized.

When these vortices with their axes parallel to the main flow are in the shear flow on the flat plate, they carry the fluid of the upper and faster portions downward on their one half side and the lower and slower portions upward on another half side, so there occur the peaks and valleys in the profiles. These processes are illustrated in Fig. 7. The shape of the resulted profile qualitatively coincides with that of the profiles in Fig. 3 (a). In downstream region, the photographs (Fig. 3 (b)) show distinctly two trailing vortex filaments in the middle, but does not show the horseshoe vortex filaments any longer, and correspondingly the velocity profile takes the form as if there are only two

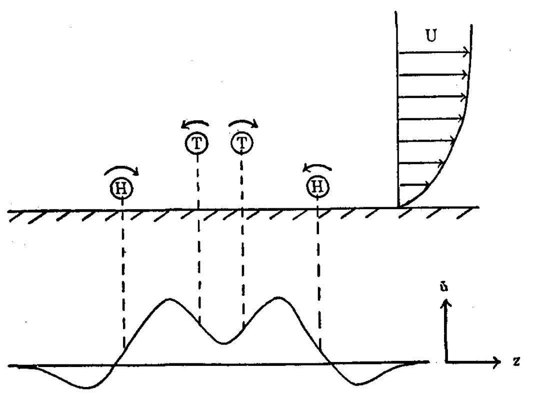

Fig. 7. Distribution of vortices and resulted velocity profiles
T: Trailing vortex,
H: Horseshoe vortex

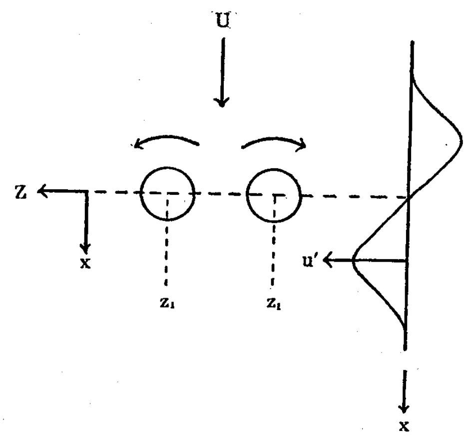

Fig. 8. Distribution of arch-shaped vortices at their legs and resulted velocity profile along $z = z_1$ or z_2

vortices in the middle.

In the second stage, Fig. 4 shows that the profile takes the same form as in the first stage, but the absolute value of the velocity difference becomes larger than in the former stage. In this stage, the horseshoe vortex filament waves three dimensionally and seems to rotate about x-axis. When only the $\bar{u}$-component of such motion is considered, the filament is regarded just as the vortex considered in the first stage. Moreover, the vortices which rise periodically from the trailing vortex filaments, i. e. arch-shaped vortices, are recognized. The legs of these vortices rotate in the direction shown in Fig. 8 which is a cross section by a plane parallel to the plate, and the tops of them rotate in such a way as the upper portion moves in the same direction to that of the main flow. As these vortices are in the wake of the sphere, the velocity near the leg on inner side of the wake is lower than that on outer side, and the velocity of the upper portion of the top is higher than that of the lower portion. So these vortices act chiefly to change periodically, the velocity in flow direction. At present, the periodic effect of these vortices cannot be observed, because only $\bar{u}$-component being measured.

In the downstream region, these periodic motions of the horseshoe vortex and the trailing vortices become weak, and the uneveness in the velocity profile becomes smooth.

In the third stage, the photographs of the smoke pattern show distinctly the turbulent region behind the sphere and the laminar region outside of it. At the boundary of the two regions, we can see the smoke filaments gather one after another and take winded forms and then become obscure by strong mixing downstream. This state indicates that there might be a longitudinal vortex near the boundary. The measurements of the mean velocity profiles show clearly that a pair of longitudinal vortices appears outside of the four longitudinal vortices existing already, just at the boundaries of the turbulence wedge, and much closer to the flat plate than the former vortices. Namely, although there are only two peaks in Figs. 3 and 4, there are four in Fig. 5. The most external slopes of the profile which ascend toward the center of the flow and are closest to the plate correspond to the boundary of the wedge where the smoke lines wind themselves.

Considering the action of the longitudinal vortices which exchange the fluid of the upper and faster portion with that of the lower and slower portion, the arrangement of the vortices like Fig. 9 seems to be probable.

If the order of the rotating directions of these vortices is considerd in z-direction, the exterior vortices are in wrong order compared with the other four. Fig. 5 (a), (b), (c), (d) show that the exterior vortices always exist on the boundary of the wedge whose region spreads down-

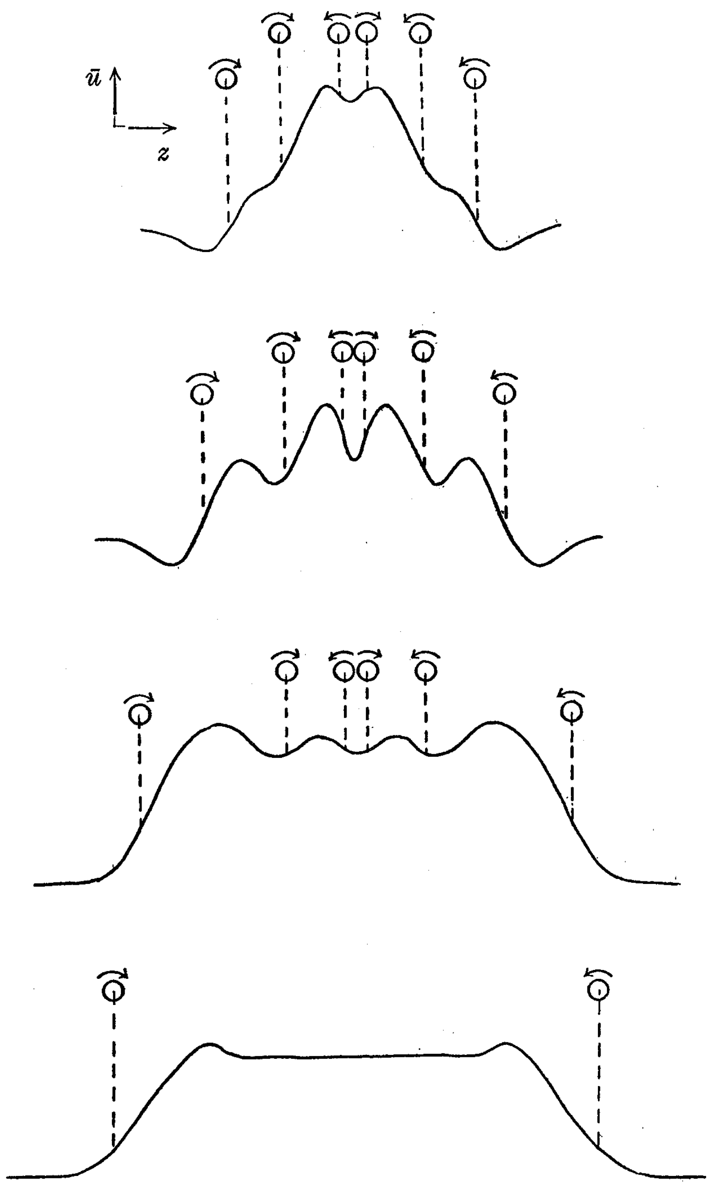

Fig. 9. Distribution of vortices and resulted velocity profiles.

downstream. Accordingly, these vortices are independent of the two kinds of the interior vortices which exist already in the second stage and are produced directly by the sphere. These are close to the plate and act to increase the velocity of the lower part of the wake. When the wind velocity increases or observations are made at farther downstream, the velocity difference between upper parts and lower ones in the wedge becomes considerably smaller (Fig. 6).

As described above, by simultaneous observation of the smoke patterns and the mean velocity profiles, we can notice that the energy of the the fluid in the upper and faster parts exchange with that in the lower and slower ones chiefly by the longitudinal vortices, and the equalization of the velocities is taken place.

The velocity fluctuation and vortices

The smoke patterns which show the fine vertex-row in the second stage are now compared to the wave forms of the hot-wire oscillograms. The hot-wire is fixed at about 9 cm downstream of the sphere on the x-position, and it is moved every 1 mm in z-direction and every 2 mm in y-direction from 0.5 mm to 11 mm. At each position the wave forms of the fluctuations are photographed for several seconds and at the same time the smoke patterns of the flow and the hot-wire are photographed stereographically by a standard-size movie camera. Some

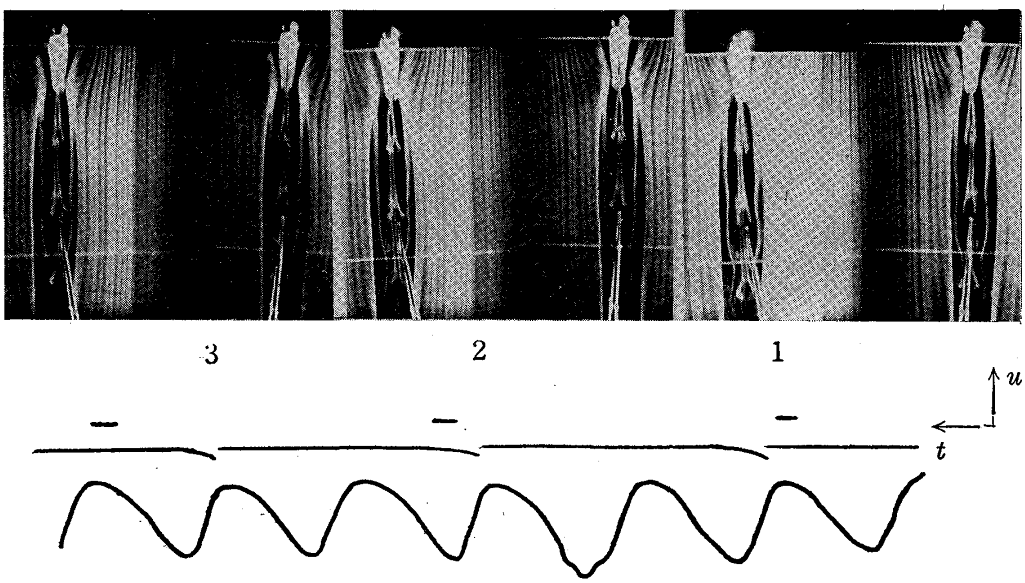

Fig. 10. Stereographs and corresponding oscillograms

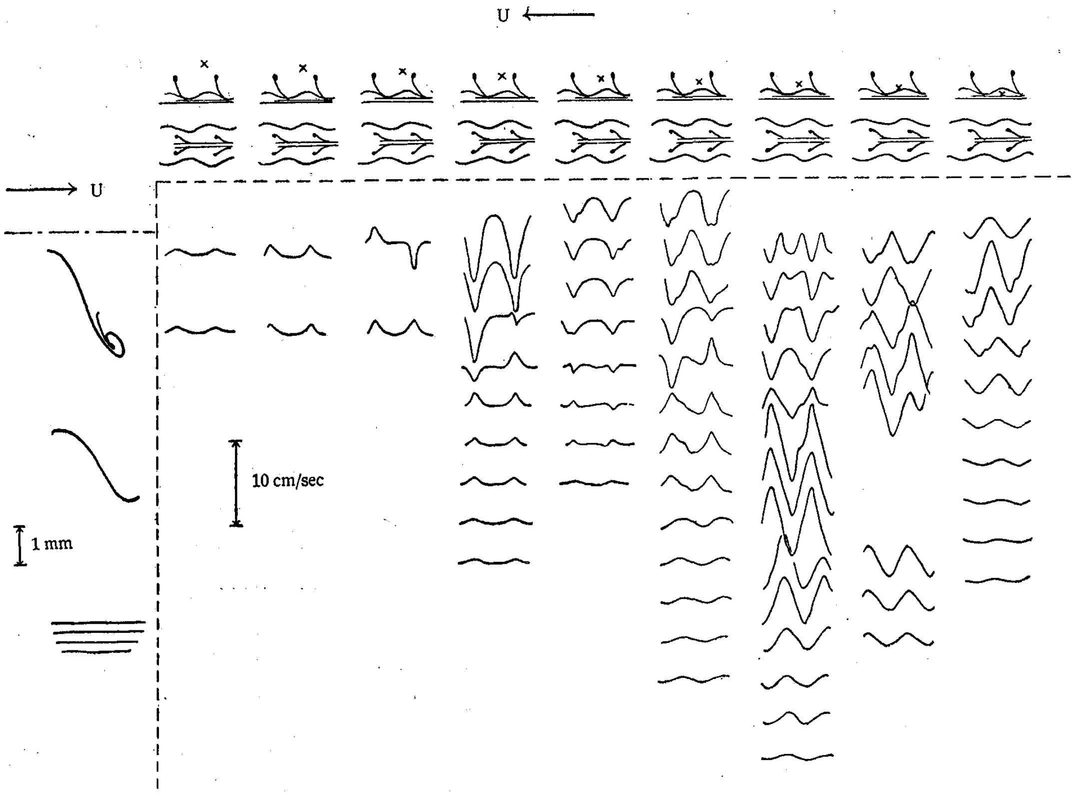

Fig. 11. Wave forms of oscillograms and corresponding positions of hot-wire relative the flow patterns

examples are shown in Fig. 10. The pulses in the middle record of the oscillogram show the instant when the exposure of each picture of the movie camera is made. Fig. 11 is the graph in which the wave forms in about two wave lengths are compared to respective position of the flow patterns. In this figure, each horizontal row corresponds to a fixed y-position of the hot-wire, and every step downward in the row indicates z-position which moves every 1 mm from the center. The top picture is the sketch of the side view of the flow pattern and the mark × shows the relative height of the hot-wire. The second picture and the left side one are the sketches of the plan-view of the flow patterns. The position of the central line of each wave form corresponds to the z-position of the hot-wire relative to the flow patterns which are on the left side of the figure.

In the second stage, it has been varified by the measurement of mean velocity that the smoke filaments of the trailing vortices indicate the central lines of the longitudinal vortices, but as for the horseshoe vortex, it has not been made clear yet whether the horseshoe vortex is cylindrical and longitudinal vortex and the smoke filaments merely wind spirally round them, or the horseshoe vortices set themselves in the spiral motion. If the former state is true, there may be no fluctuation in u-component. It is noticed from Fig. 11, however, that the phase of the wave forms at the same x-and y-positions differs on both lateral sides of the vortex, and the wave forms at the upper positions of the vortex are reversed to those at the lower positions. From these facts it is concluded that the horseshoe vortex sets itself in the spiral motion in the direction indicated in Fig. 7.

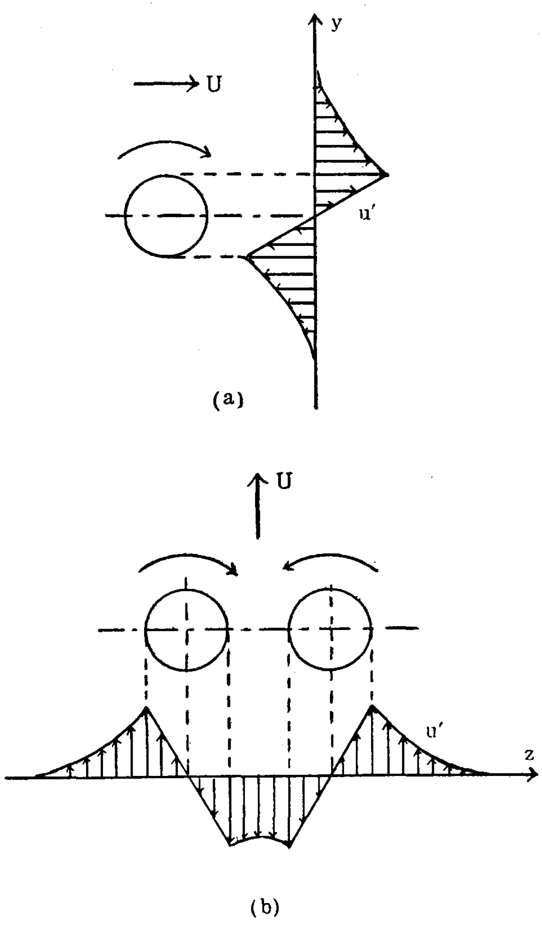

Fig. 12. Profiles of velocity fluctuations caused by (a) a single and (b) a pair of circular vortices

Now, the arch-shaped vortices which have not been observed by the measurements of the mean velocity profiles are considered. If we assume that these vortices are the circular ones whose vorticity is uniform over a cross section and, accordingly, the velocity profiles take forms like Fig. 12, the wave forms of Fig. 11 can be explained. For example, the wave forms above the top of the vortices are reversed to those below it as expected from Fig. 12 (a). At the leg of the vortices, the velocity fluctuations become smaller between the two legs, and the wave forms are reversed on both sides of a leg (Fig. 12 (b)).

As the size of each arch-shaped vortex varies in some extent, in some positions of the hot-wire where the vortices of mean size may pass over, the position of the hot-wire becomes outside or inside of respective vortex as its size is smaller or larger, therefore, the wave forms may reverse their signs as the size of the vortex varies.

Conclusion

As it has been pointed out in former paper[1] that the smoke pattern differs as the position of the smoke source changes relative to the existing vortices. However, according to the present observed results using the smoke method and the hot-wire method simultaneously, each smoke pattern can be regarded to express faithfully the respective pattern of the flow. It is further verified that the smoke gathers in the central of the vortices and consequently the smoke filaments indicate the central parts of the vortices and, moreover, the smoke pattern can distinguish the laminar region and the turbulent one.

The velocity profiles in the downstream region of the roughness can be explained chiefly by the effects of the longitudinal vortices which transfer the faster fluid elements downward and the slower ones upward. In the turbulent state the vortices in the middle part of the turbulence wedge disappear and the profiles become flat in z-direction and considerably smaller in y-ward differences. There exist the longitudinal vortices on the boundary of the wedge and they cause a steep change of the velocity between outer and inner region of the wedge.

The author wishes to express her cordial thanks to Prof. Jiro Sakagami for his kind guidance and constant encouragement throughout the course of this investigation. She is also grateful to the members of the Boundary Layer Research Group directed by Prof. Itiro Tani for their helpful discussions.

References

1) Mochizuki, M.: Some Observation on Boundary Layer Transition Caused by a Spherical Roughness Element., Jour. Phys. Soc. Japan, **16** (1961), p. 995.
2) Schubauer, G. B. and Klebanoff, P. S.: Contribution on the Mechanics of Boundary-Layer Transition, NACA Rep. 1289 (1956).
3) Tani, I.: To be published in the Rep. Aero. Res. Inst., Univ. of Tokyo.
4) Gregory, N. and Walker, W. S.: The Effect on Transition of Isolated Surface Excrescences in the Boundary Layer, A. R. C. Tech. Rep., 13436 (1950).
5) Weske, J. R.: Experimental Study of Detail Phenomena of Transition in Boundary Layers., Tech. Note, BN-91, Inst. Fluid Dyn. and Appl. Math., Univ. Marryland (1957).
6) Taneda, S.: Experimental Investigation of the Wake behind a Sphere at Low Reynolds Numbers., Jour. Phys. Soc. Japan, **11** (1956), p. 1104.
7) Schubauer, G. B.: Mechanism of Transition at Subsonic Speeds., "Boundary Layer Research," IUTAM Symposium in Freiburg 1957, Springer-Verlag, 1958, p. 85.

(*Received August 1, 1961*)